molecules

MDPI

Article

Ultrasound-Assisted Extraction of Polyphenols from *Hericium erinaceus*: Optimization, Bioactivities and LC-MS-Based Chemical Profiling

Hongfei Liu [1,2,†], Cong Zhao [3,†], Shuyue Pang [1,2], Yuting Shu [1,2], Lina Chen [1,2], Jing Wang [1,2,3,*] and Helong Bai [1,*]

[1] College of Chemistry, Changchun Normal University, Changchun 130032, China; qx202308010@stu.ccsfu.edu.cn (H.L.); qx202308024@stu.ccsfu.edu.cn (S.P.); qx202408003@stu.ccsfu.edu.cn (Y.S.); chenlina4321@163.com (L.C.)
[2] Institute of Science and Technology Innovation, Changchun Normal University, Changchun 130032, China
[3] College of Life Sciences, Changchun Normal University, Changchun 130032, China; zhaocong@ccsfu.edu.cn
* Correspondence: wangjing018@ccsfu.edu.cn (J.W.); baihelong@ccsfu.edu.cn (H.B.)
† These authors contributed equally to this work.

Abstract

In this study, the Box–Behnken Design (BBD) was adopted to optimize the ultrasound-assisted extraction (UAE) conditions of polyphenols from *Hericium erinaceus* (*H. erinaceus*) on the basis of single-factor experiments, with extraction time, solid–liquid ratio and ethanol concentration as the key investigation factors. The optimal extraction parameters were determined as follows: extraction time of 56.85 min, solid–liquid ratio of 1:56.71 g/mL and ethanol concentration of 44.64%, under which the actual yield of the total polyphenol crude extract (TPCE) reached 0.9985 ± 0.03%, which was highly consistent with the theoretical predicted value of 0.9960%, verifying the good fitting degree of the established model. Taking L-ascorbic acid as the positive control, the antioxidant activity of TPCE was evaluated by determining its scavenging capacity against ABTS·$^{+}$, ·OH and DPPH· free radicals, and the half-maximal effective concentration (EC_{50}) values were measured to be 0.8850, 0.9490 and 4.198 mg/mL, respectively. With acarbose as the reference drug, the inhibitory effects of TPCE on α-amylase and α-glucosidase related to carbohydrate metabolism were assayed, and the corresponding half-maximal inhibitory concentration (IC_{50}) values were 0.0135 and 130.3 mg/mL, respectively. Furthermore, ultra-high performance liquid chromatography-quadrupole time-of-flight mass spectrometry (UHPLC-QTOF-MS) was employed for the tentative identification of bioactive components in TPCE, and a total of 48 and 64 chemical constituents were characterized in negative and positive ion modes, respectively, providing a chemical basis for the biological activities of TPCE. This study confirmed that UAE is an efficient and feasible technology for extracting polyphenols from *H. erinaceus*, which lays a theoretical foundation for the development and utilization of its polyphenols, and also provides novel insights into the development of natural functional ingredients and potential therapeutic agents for the intervention of type 2 diabetes. Additionally, the findings further validate edible fungi as a valuable reservoir of natural bioactive substances, with promising application prospects in the research and development of functional foods and pharmaceuticals targeting metabolic diseases.

Keywords: *Hericium erinaceus*; extraction optimization; antioxidant activity; α-amylase; α-glucosidase

Check for updates

Academic Editor: Claudio Ferrante

Received: 3 March 2026
Revised: 25 March 2026
Accepted: 27 March 2026
Published: 30 March 2026

Copyright: © 2026 by the authors. Licensee MDPI, Basel, Switzerland. This article is an open access article distributed under the terms and conditions of the Creative Commons Attribution (CC BY) license.

1. Introduction

Edible mushrooms are widely appreciated for their nutritional properties, as well as for their biological activities and therapeutic potential. Regarding medicinal values, mushrooms have emerged as an important source of compounds with antioxidant, antimicrobial and antitumor features [1]. *H. erinaceus* has historically been broadly cultivated and widely consumed as traditional medicinal herbs as well as functional food in the orient for several hundred years [2]. Members of the genus *H. erinaceus* produce fleshy, whitish basidiomata, such as *H. erinaceus* coralloides (Scop.) Pers. (in *Hericiaceae*, Russulales, Agaricomycetes, Basidiomycota) [3]. It is distributed across the Northern Hemisphere in Europe, Asia and North America [4]. There are 73 records in the Fungus Index (http://www.indexfungorum.org/Names/NAMES.ASP (accessed on 26 March 2026)), indicating that *H. erinaceus* is rich in a variety of functional active ingredients, with various physiological functions such as anticancer and enhancing immunity [5]. Studies have shown that, in addition to functional macromolecules such as polysaccharides and proteins, *H. erinaceus* also contains small molecular active components such as terpenoids, cerebrosides, phenols and sterols [4]. These bioactive compounds have various physiological activities in healthcare functions [6].

Plant polyphenols, secondary metabolites in plants, possess valuable functional properties, including anti-inflammatory, antioxidative and hypoglycemic effects [7]. These substances vary from simple molecules to complex structures, all featuring benzenic rings with two or more hydroxy groups. These active components are essential for development, fertility, and immunity against infections, pathogens, and diseases. Polyphenolic compounds are naturally occurring biologically active compounds that have been thoroughly researched due to their beneficial impact on health [8,9]. In addition to their therapeutic roles, polyphenols contribute to the taste, appearance, and organoleptic characteristics of foods [10]. A variety of compounds have been identified in *H. erinaceus* across different studies, including acetohydroxamic acid, catechin hydrate, resveratrol, myricetin, fumaric acid, gallic acid, protocatechuic acid, 4-hydroxybenzoic acid, phloridzin dihydrate, 2-hydroxycinnamic acid, naringenin, quercetin, and luteolin [11]; 3,4-dihydroxybenzoic acid, caffeic acid, syringic acid, rutin, ellagic acid, p-coumaric acid, salicylic acid, vanillin, ferulic acid, sinapic acid, rosmarinic acid, and t-cinnamic acid [12]; α-resorcylic acid and 4-coumaric acid [13]; as well as succinic acid, catechin, and 2-hydroxybenzoic acid [14]. Based on the above, it is necessary to conduct in-depth research on polyphenols from *H. erinaceus*.

The use of ultrasound-assisted extraction (UAE) of bioactive compounds has been in-creasing because it is a good alternative to the conventional extraction methods. UAE was used to maximize total polyphenol content [15,16]. Also, two primary systems have been widely employed in ultrasonic extraction: ultrasonic probes and ultrasonic baths. Previous studies have demonstrated that ultrasonic probes exhibit superior efficiency in extracting active components [17], while ultrasonic baths offer the advantage of protecting the structural integrity and biological activity of target active substances throughout the extraction process [18]. The selection of extraction solvent for ultrasonic-assisted extraction is also critically important. Although methanol has been reported to be the optimal solvent for extracting total phenolic compounds from *G. applanatum* and *F. fomentarius*, ethanol was still employed as the extraction solvent in this study. Distinct from the commonly used methanol, ethanol is classified as a GRAS (Generally Recognized as Safe) solvent, which constitutes the core reason for selecting ethanol as the extraction solvent in the present experiment [19,20].

Type 2 diabetes mellitus and its related complications are growing public health problems. Many natural products including polyphenols can be used in treating and managing

type 2 diabetes mellitus and different diseases, owing to their numerous biological properties [21]. Controlling carbohydrate digestibility by inhibiting starch digestive enzyme (α-amylase and α-glucosidase) activities is an efficient strategy to control postprandial hyperglycemia [22]. Hyperglycemia in DM is known to increase reactive oxygen species production, enhancing oxidative stress and glycation, which in turn contributes to the development of advanced glycation end products, exacerbating diabetic complications [23]. The potent antioxidant capabilities of polyphenols can help battle oxidative stress, one of the key factors in the pathogenesis of diabetes. Although *H. erinaceus* contains phenolic components and exhibits diverse physiological activities, studies on its polyphenol extraction, antioxidant and enzyme inhibitory activities, as well as their links to hypoglycemic effects, remain limited and insufficient.

In order to fully explore the potential of *H. erinaceus* polyphenols as natural antioxidants and hypoglycemic active substances, and fill the research gap in this field, polyphenols yield was used as the core evaluation index in the present study to optimize the extraction process of polyphenols from *H. erinaceus*. On this basis, the antioxidant activity and starch digestive enzyme inhibition activity of the extracted polyphenol components were systematically investigated, aiming to provide experimental data and theoretical support for the in-depth development and utilization of *H. erinaceus* as a functional food resource for the prevention and auxiliary treatment of type 2 diabetes mellitus.

2. Results and Discussion

2.1. Optimization of Polyphenol Extraction Procedure

2.1.1. Effect of Different Factors on Polyphenol Yield

The relationship between the concentration of gallic acid (x) and absorbance (y) fitted the standard curve: $y = 3.8469x + 0.0075$. Polyphenol content was calculated based on this regression. The polyphenol content initially increased, then decreased with a rising solid–liquid ratio. The highest polyphenol content was achieved at a solid–liquid ratio of 1:50, after which it continuously declined with further increasing solid–liquid ratio (Figure 1a). This may be attributed to the fact that a low solid–liquid ratio restricts sufficient contact between the sample and the solvent, while an excessively high ratio may increase the dissolution of impurities and even cause the degradation of polyphenols [24]. Extraction time significantly impacted polyphenol dissolution, reaching its peak at 50 min. At this point, polyphenol was mostly dissolved, and extending the ultrasonic time beyond 50 min resulted in decreased polyphenol content (Figure 1b). This may be attributed to the loss of target bioactive components caused by excessive extraction. The effect of ethanol concentration on polyphenol extraction yield follows a similar pattern, peaking at 40% ethanol concentration. Beyond this point, the polyphenol content decreases consistently (Figure 1c). As documented by Rahimah et al., 40% ethanol offers the optimal polarity for recovering phenolic compounds from edible mushrooms, as higher ethanol levels increase the solubility of unwanted macromolecules and reduce the extraction selectivity for polyphenols [25].

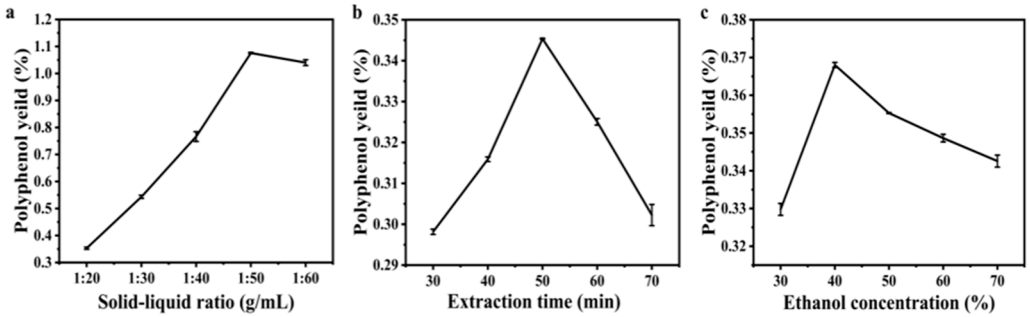


Figure 1. Effects of different factors on ultrasonic extraction of polyphenol from *H. erinaceus*. (**a**). Effect of solid–liquid ratio on polyphenol yield; (**b**). Effect of extraction time on polyphenol yield; (**c**). Effect of ethanol concentration on polyphenol yield.

2.1.2. Polyphenol BBD Analysis

The extraction temperature, extraction time and solid–liquid ratio were further optimized by BBD based on the results of single-way experiments. Table 1 shows the experimental data of BBD under different combinations of extraction conditions. Table 2 shows the results of ANOVA. Accordingly, the second-order polynomial equation was established as follows:

$$Y = -9.16012 + 0.123691 \times A + 0.143075 \times B + 0.162185 \times C - 0.0001375 \times A \times B - 7.5 \times 10^{-5} \times A \times C + 3 \times 10^{-5} \times B \times C - 0.0014058 \times A^2 - 0.0013893 \times B^2 - 0.0015433 \times C^2$$

Table 1. BBD experimental results.

Number	A: Extraction Time (min)	B: Solid–Liquid Ratio (g/mL)	C: Ethanol Concentration (%)	Polyphenol Yield (%)
1	60	50	30	0.8399
2	40	40	40	0.7616
3	50	50	40	1.1139
4	50	40	30	0.7458
5	50	60	30	0.8965
6	50	40	50	0.7682
7	60	50	50	0.8291
8	40	60	40	0.8741
9	50	50	40	1.1038
10	40	50	30	0.8239
11	40	50	50	0.8681
12	60	40	40	0.7729
13	50	50	40	1.1309
14	60	60	40	0.8974
15	50	50	40	1.1305
16	50	60	50	0.8889
17	50	50	40	1.1197

Table 2. Regression equation model and analysis of variance.

Source	Sum of Squares	df	Mean Square	F-Value	*p*-Value
Model	0.3294	9	0.0366	225.88	<0.0001 ***
A	0	1	0	0.1038	0.7567
B	0.0323	1	0.0323	199.37	<0.0001 ***
C	0.0003	1	0.0003	1.79	0.2225
AB	0	1	0	0.2221	0.6517
AC	0.0008	1	0.0008	4.67	0.0676
BC	0.0002	1	0.0002	1.39	0.2772
A^2	0.0813	1	0.0813	501.49	<0.0001 ***
B^2	0.1003	1	0.1003	618.83	<0.0001 ***
C^2	0.0832	1	0.0832	513.47	<0.0001 ***
Residual	0.0011	7	0.0002		
Lack of Fit	0.0006	3	0.0002	1.53	0.3369
Pure Error	0.0005	4	0.0001		
Cor Total	0.3306	16			
				R^2	0.9966
				R^2 Adj	0.9922
				R^2 Pre	0.9682
				Adeq Precision	38.0992

Note: *** indicates extremely significant differences, $p < 0.001$.

From Table 2, it is evident that the model's regression is highly significant ($p < 0.0001$), with a lack of fit of 0.3369, exceeding the significance threshold of 0.05. This indicates a strong model fit, capable of depicting the relationship between the response value and various factors. ANOVA showed that the model was significant, while the linear term of extraction time (A) was insignificant ($p = 0.7567$). Primary items B, along with secondary factors A^2, B^2 and C^2, exhibited extremely significant differences. The effects of the three factors on polyphenol extraction ranked as follows: Solid–liquid ratio (B) > Ethanol concentration (C) > Extraction time (A). This ranking was observed despite the insignificance of the linear term for A, which could be attributed to the highly significant quadratic term (A^2, $p < 0.0001$) masking the non-significance of its linear term.

2.1.3. Interactions in BBD Experiments of Polyphenol Extraction

Based on the fitted equations, three-dimensional response surface plots of different factors on the composite scores were developed using Design-Expert 8.0.6 software.

As shown in Figure 2, the interaction between the polyphenol extraction variables was visualized on a three-dimensional surface reflecting the combined effect of a number of factors on the response values when they intersect. Figure 2A shows that when the ethanol concentration remained constant, the yield first increased with increasing extraction time. After the highest yield was reached, the yield decreased with increasing extraction time; the yield increased and then decreased as the solid–liquid ratio increased. Figure 2B shows that when the solid–liquid ratio was constant, the polyphenol yield first showed a rapid upward trend with increasing extraction time. When the extraction time increased to a certain value, the polyphenol yield decreased immediately; the polyphenol yield decreased with increasing ethanol concentration. Figure 2C shows that when the extraction time was constant, the polyphenol yield first increased and then decreased with increasing solid–liquid ratio and the ethanol concentration increased; the polyphenol yield first increased, but after the highest peak was reached, the yield decreased with the solid–liquid ratio. The results show that the response surface plot for AC is steeper for this interaction term, indicating that AC has a significant effect on the composite score.

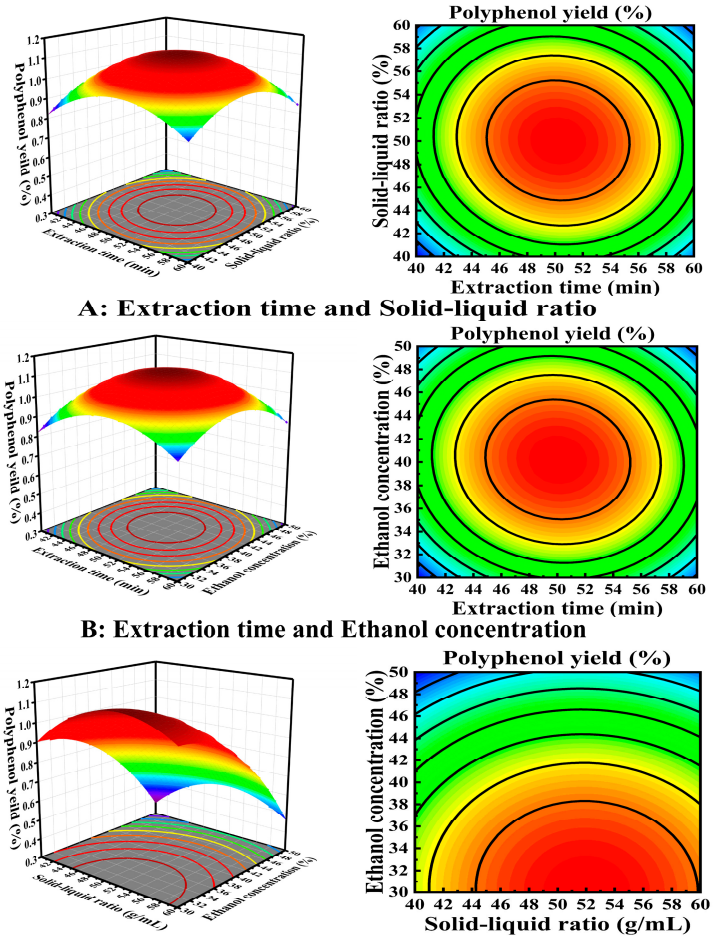


Figure 2. Response Surface and contour map of interaction between three factors affecting *H. erinaceus* polyphenol extraction content.

2.1.4. Experimental Verification of Polyphenol Extraction

The optimal extraction conditions of polyphenol from *H. erinaceus* were obtained by the Box–Behnken experiment, under the extraction conditions of extraction time 56.85 min, solid–liquid ratio 1:56.71 g/mL, and ethanol concentration 44.64%; the theoretical prediction value of polyphenol yield was 0.9960%. We repeated the experiment three times under those conditions, and the average polyphenol yield from *H. erinaceus* was 0.9985 ± 0.03%, which is basically consistent with the predicted value and further verifies the feasibility of the theoretical model. Notably, the targeted components in this extraction study mainly comprised polyphenolic compounds (such as protocatechuic acid, gallic acid, p-coumaric acid) from *H. erinaceus*, and the optimized conditions were precisely screened to enable efficient extraction of these bioactive substances.

2.2. Analysis of the Extracts by LC-MS

The crude extract of *H. erinaceus* was analyzed using LC-MS with electrospray ionization. Figure 3 shows the spectra for both positive and negative ion modes.

By comparing the acquired high-resolution mass spectrometry data against an established spectral library, 48 and 64 chemical constituents in negative ion modes (Table 3) and positive ion modes (Table 4) were tentatively identified, respectively. These constituents cover multiple compound classes, including primary metabolites such as sugar alcohols, organic acids, free amino acids, and small peptides, as well as lipid components including glycerophospholipids, fatty acids and their oxidized derivatives, together with several

terpenoids, steroids and mushroom-specific bioactive components. In addition, compounds including D-arabitol, D-(+)-malic acid, and uridine diphosphate-N-acetylglucosamine are consistent with the results reported by Sevindik [11]. The results confirm the presence of multiple bioactive compounds in the extract, though their specific biological functions remain to be further validated experimentally.

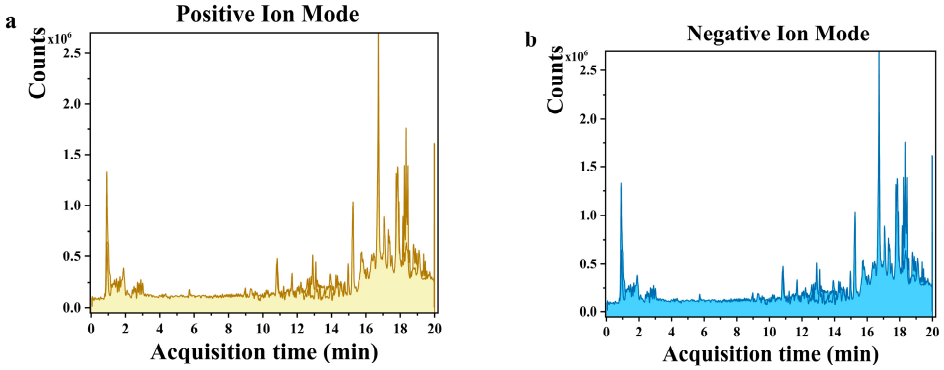


Figure 3. Positive and negative ion mode spectra. (**a**) Positive ion mode spectra; (**b**) negative ion mode spectra.

Table 3. Results of the negative ion modes.

NO.	Retention Time (min)	Mass-to-Charge Ratio (*m*/*z*)	Name	Formula
1	0.877	227.0775	L-Iditol	$C_6H_{14}O_6$
2	0.903	487.1816	Ala His Met Met	$C_{19}H_{32}N_6O_5S_2$
3	0.908	181.0728	Lathyrine	$C_7H_{10}N_4O_2$
4	0.922	573.1516	Cys Asp Glu Tyr	$C_{21}H_{28}N_4O_{10}S$
5	0.932	355.0936	5-Hydroxy-4-methoxy-3-methyl-2,6-canthinedione	$C_{16}H_{12}N_2O_4$
6	0.934	231.0311	9-Hydroxy-4-methoxypsoralen	$C_{12}H_8O_5$
7	0.94	387.1175	Fructoselysine 6-phosphate	$C_{12}H_{25}N_2O_{10}P$
8	0.945	311.1028	Flurprimidol	$C_{15}H_{15}F_3N_2O_2$
9	0.966	439.0866	3,5-Dihydroxyphenyl 1-O-(6-O-galloyl-beta-D-glucopyranoside)	$C_{19}H_{20}O_{12}$
10	0.97	151.062	D-Arabitol	$C_5H_{12}O_5$
11	1.017	133.0154	D-(+)-Malic acid	$C_4H_6O_5$
12	1.026	267.0742	cis-ACCP	$C_7H_{15}N_2O_4P$
13	1.065	606.0768	Uridine diphosphate-N-acetylglucosamine	$C_{17}H_{27}N_3O_{17}P_2$
14	1.074	191.021	Citric acid	$C_6H_8O_7$
15	1.345	191.0201	2,3-Dioxogulonic acid	$C_6H_8O_7$
16	1.477	231.0159	6-Cyano-7-nitroquinoxaline-2,3-dione	$C_9H_4N_4O_4$
17	1.673	115.0039	Formylpyruvate	$C_4H_4O_4$
18	10.804	740.4941	PS(P-16:0/18:3(9Z,12Z,15Z))	$C_{40}H_{72}NO_9P$
19	12.616	429.1565	Thr His Cys Ala	$C_{16}H_{26}N_6O_6S$
20	12.863	429.1562	17β-hydroxy Wortmannin	$C_{23}H_{26}O_8$
21	13.911	331.156	Gibberellin A20	$C_{19}H_{24}O_5$
22	14.731	415.1771	Erioflorin methacrylate	$C_{23}H_{28}O_7$
23	15.716	293.212	alpha-kamlolenic acid	$C_{18}H_{30}O_3$
24	15.733	295.2283	9(R)-HODE	$C_{18}H_{32}O_3$
25	15.982	265.1486	Lauryl hydrogen sulfate	$C_{12}H_{26}O_4S$
26	16.378	564.3322	PE(20:2(11Z,14Z)/0:0)	$C_{25}H_{48}NO_7P$
27	16.547	459.2976	Lys Lys Ser Val	$C_{20}H_{40}N_6O_6$
28	16.615	489.3084	Phe Ile Ile Val	$C_{26}H_{42}N_4O_5$
29	16.724	333.2295	9,10-dihydroxy-hexadecanoic acid	$C_{16}H_{32}O_4$
30	16.74	379.2376	Emopamil	$C_{23}H_{30}N_2$
31	16.764	279.2338	9(E),11(E)-Conjugated Linoleic Acid	$C_{18}H_{32}O_2$
32	16.787	459.3003	Eicosapentaenoyl Serotonin	$C_{30}H_{40}N_2O_2$

Table 3. *Cont.*

NO.	Retention Time (min)	Mass-to-Charge Ratio (*m*/*z*)	Name	Formula
33	16.813	311.1691	N-Undecylbenzenesulfonic acid	$C_{17}H_{28}O_3S$
34	16.936	339.2334	1,1′-[1,11-Undecanediylbis(oxy)]bisbenzene	$C_{23}H_{32}O_2$
35	17.116	435.2983	Termitomycamide B	$C_{28}H_{40}N_2O_2$
36	17.31	669.5314	Glycerol 1-dodecanoate 2-tetradecanoate 3-octanoate	$C_{37}H_{70}O_6$
37	17.317	281.2494	C18:1n-13	$C_{18}H_{34}O_2$
38	17.372	451.2842	PA(19:0/0:0)	$C_{22}H_{45}O_7P$
39	17.407	461.3134	Sorbitan palmitate	$C_{22}H_{42}O_6$
40	17.581	325.1848	4-Dodecylbenzenesulfonic acid	$C_{18}H_{30}O_3S$
41	17.766	279.235	Linoleic acid	$C_{18}H_{32}O_2$
42	17.793	413.1007	Dihydrogriseofulvin	$C_{17}H_{19}C_1O_6$
43	17.845	293.1802	Sodium Tetradecyl Sulfate	$C_{14}H_{30}O_4S$
44	17.926	407.2488	Dimethamine	$C_{24}H_{32}N_4O_2$
45	18.393	323.2209	TOFA	$C_{19}H_{32}O_4$
46	18.408	255.2335	Palmitic Acid	$C_{16}H_{32}O_2$
47	18.786	415.1156	BAY-u3405	$C_{21}H_{21}FN_2O_4S$
48	19.453	319.2321	20-HETE	$C_{20}H_{32}O_3$

Table 4. Results of the positive ion modes.

NO.	Retention Time (min)	Mass-to-Charge Ratio (*m*/*z*)	Name	Formula
1	0.86	104.106	Choline	$C_5H_{14}NO$
2	0.971	148.0601	L-Glutamic acid	$C_5H_9NO_4$
3	1.01	258.1098	Glycerophosphocholine	$C_8H_{21}NO_6P$
4	1.064	118.0855	L-Valine	$C_5H_{11}NO_2$
5	1.689	129.0543	Methyl 4-oxo-2-pentenoate	$C_6H_8O_3$
6	1.867	132.1024	L-Leucine	$C_6H_{13}NO_2$
7	2.739	166.0851	DL-Phenylalanine	$C_9H_{11}NO_2$
8	10.841	701.4922	PC(10:0/18:0)	$C_{36}H_{73}NO_8P$
9	13.05	353.1347	Gibberellin A95	$C_{19}H_{22}O_5$
10	13.943	355.1492	Dinocton	$C_{16}H_{22}N_2O_7$
11	15.053	365.1321	Ser Ser Gly Asp	$C_{12}H_{20}N_4O_9$
12	15.17	301.1393	7-Methylinosine	$C_{11}H_{15}N_4O_5$
13	15.225	579.286	Ala Arg Asp Pro Val	$C_{23}H_{40}N_8O_8$
14	15.281	279.1563	Monomenthyl succinate	$C_{14}H_{24}O_4$
15	15.629	357.2574	8-iso Prostaglandin E2-d4	$C_{20}H_{28}D_4O_5$
16	15.668	401.2831	Arg Ile Ile	$C_{18}H_{36}N_6O_4$
17	15.723	445.3087	17-phenyl trinor Prostaglandin F2α cyclopropyl amide	$C_{26}H_{37}NO_4$
18	15.846	489.3342	(17Z)-1α,25-dihydroxy-26,27-dimethyl-17,20,22,22,23,23-hexadehydro-24a,24b-dihomovitamin D3/(17Z)-1α,25-dihydroxy-26,27-dimethyl-17,20,22,22,23,23-hexadehydro-24a,24b-dihomocholecalciferol	$C_{31}H_{46}O_3$
19	16.371	520.3338	Thr Arg Arg Ala	$C_{19}H_{38}N_{10}O_6$
20	16.384	542.3155	Asn Pro Arg Arg	$C_{21}H_{39}N_{11}O_6$
21	16.393	639.3999	PA(18:2(9Z,12Z)/12:0)	$C_{33}H_{61}O_8P$
22	16.435	595.3745	PS(22:2(13Z,16Z)/0:0)	$C_{28}H_{52}NO_9P$
23	16.553	437.2822	*Hericerin*	$C_{27}H_{33}O_3$
24	16.592	385.2883	Kalkitoxin thioamide alcohol	$C_{21}H_{40}N_2O_2S$
25	16.598	399.2676	10′-apo-beta-carotenal	$C_{27}H_{36}O$
26	16.615	473.3394	Phylloquinone	$C_{31}H_{46}O_2$

Table 4. *Cont.*

NO.	Retention Time (min)	Mass-to-Charge Ratio (*m*/*z*)	Name	Formula
27	16.709	341.2626	12-epi Leukotriene B4-d4	$C_{20}H_{28}D_4O_4$
28	16.712	429.3139	Fesoterodine	$C_{26}H_{37}NO_3$
29	16.722	781.5185	PI(P-18:0/13:0)	$C_{40}H_{77}O_{12}P$
30	16.734	357.2218	(R,E)-S-2-acetamido-13-(methylamino)-13-oxotridec-3-enyl ethanethioate	$C_{18}H_{32}N_2O_3S$
31	16.753	693.4676	PG(12:0/18:1(9Z))	$C_{36}H_{69}O_{10}P$
32	16.766	605.4164	PA(17:1(9Z)/12:0)	$C_{32}H_{61}O_8P$
33	16.775	737.4934	PC(18:3(9Z,12Z,15Z)/13:0)	$C_{39}H_{73}NO_8P$
34	16.792	437.2832	Pangamic acid	$C_{20}H_{40}N_2O_8$
35	16.866	425.2824	Lys Lys Lys	$C_{18}H_{38}N_6O_4$
36	16.874	413.2824	1α-fluoro-25-hydroxy-16,17,23,23,24,24-hexadehydrovitamin D3/1α-fluoro-25-hydroxy-16,17,23,23,24,24-hexadehydrocholecalciferol	$C_{27}H_{37}FO_2$
37	16.888	522.3488	Dipyridamole	$C_{24}H_{40}N_8O_4$
38	17.102	439.2978	Apo-8′-lycopenal	$C_{30}H_{40}O$
39	17.501	629.4884	1-(6-[5]-ladderane-hexanyl)-2-(8-[3]-ladderane-octanyl)-sn-glycerol	$C_{41}H_{66}O_3$
40	17.646	457.3445	N-arachidonoyl vanillylamine	$C_{28}H_{41}NO_3$
41	17.665	427.2985	Leupeptin	$C_{20}H_{38}N_6O_4$
42	17.667	501.3704	Deterrol stearate	$C_{33}H_{50}O_2$
43	17.689	589.422	Arg Arg Leu Lys	$C_{24}H_{49}N_{11}O_5$
44	17.788	809.5503	PI(P-20:0/13:0)	$C_{42}H_{81}O_{12}P$
45	17.797	853.5748	PS(22:6(4Z,7Z,10Z,13Z,16Z,19Z)/18:0)	$C_{46}H_{78}NO_{10}P$
46	17.798	721.4987	PG(14:0/18:1(9Z))	$C_{38}H_{73}O_{10}P$
47	17.804	585.4637	3,4-Dihydrospheroidenone	$C_{41}H_{60}O_2$
48	17.804	765.5238	Spinetoram	$C_{42}H_{69}NO_{10}$
49	17.832	435.3627	Petrosterol	$C_{29}H_{48}O$
50	17.835	479.3884	2-Tricosanamidoethanesulfonic acid	$C_{25}H_{51}NO_4S$
51	17.838	677.4725	Lansioside A	$C_{38}H_{61}NO_8$
52	17.864	633.447	PA(17:0/14:1(9Z))	$C_{34}H_{65}O_8P$
53	17.867	369.2934	2,3-dinor-6-keto Prostaglandin F1α-d9	$C_{18}H_{21}D_9O_6$
54	17.875	545.396	Daphniphylline	$C_{32}H_{49}NO_5$
55	17.918	413.3194	N-Octadecyl-N′-propyl-sulfamide	$C_{21}H_{46}N_2O_2S$
56	17.944	431.2388	Deoxypyridinoline	$C_{18}H_{29}N_4O_7$
57	18.129	515.3321	Ile Leu Arg Asn	$C_{22}H_{42}N_8O_6$
58	18.256	475.3397	5beta-Cholestane-3alpha,7alpha,12alpha,23,26-pentol	$C_{27}H_{48}O_5$
59	18.37	441.3139	dolichyl phosphate	$C_{25}H_{45}O_4P$
60	18.392	401.322	4,4′-Diapolycopene	$C_{30}H_40$
61	19.09	381.2933	1′H-5alpha-Androst-2-eno[3,2-b]indol-17beta-ol	$C_{25}H_{33}NO$
62	19.101	803.5327	PE(22:6(4Z,7Z,10Z,13Z,16Z,19Z)/18:3(9Z,12Z,15Z))	$C_{45}H_{72}NO_8P$
63	19.104	413.2617	Diisooctyl phthalate	$C_{24}H_{38}O_4$
64	19.699	451.3124	N-arachidonoyl glutamic acid	$C_{25}H_{39}NO_5$

2.3. Antioxidant Activity

As depicted in Figure 4, the scavenging effects of TPCE on $ABTS^+\cdot$, ·OH, and DPPH· radicals show a concentration-dependent enhancement with increasing TPCE concentration. TPCE showed markedly different scavenging capacities toward the three free radicals. Although its scavenging activity was lower than that of Vc within the tested concentration range, TPCE is a complex mixture rather than a monomeric compound, indicating its potential for strong antioxidant activity. Specifically, EC_{50} values of TPCE for $ABTS^+\cdot$, ·OH, and

DPPH· were calculated as 0.8850 mg/mL, 0.9490 mg/mL, and 4.198 mg/mL, respectively. Compared with the reported EC_{50} values for analogous natural and edible mushroom extracts in the literature, the EC_{50} values determined in the present study fall well within the range of crude extracts with moderate antioxidant activity, except for a noticeably weaker DPPH radical scavenging capacity [26,27]. Based on LC-MS profiling, primary metabolites including D-arabitol, D-(+)-malic acid, uridine diphosphate-N-acetylglucosamine, together with terpenoids and mushroom-specific bioactive compounds, were suggested to contribute collectively to the antioxidant effects observed in this study, which was reported in the findings of Sevindik, M. et al. [11].

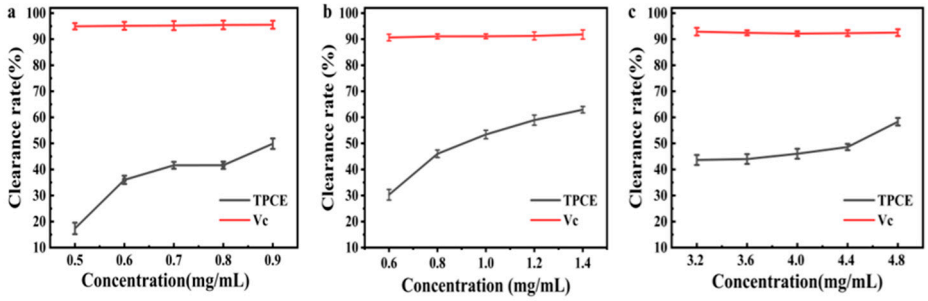


Figure 4. The scavenging activities of TPCE against three types of free radicals. (**a**) $ABTS^{+}$·, (**b**) ·OH, (**c**) DPPH·.

2.4. Enzyme Inhibitory Activity

As shown in Figure 5a, the inhibition of α-amylase by TPCE intensified with increased concentrations. The inhibition rate improved from 24.91 ± 1.31% to 69.36 ± 1.49% as TPCE concentrations increased from 0.008 to 0.020 mg/mL, with an IC_{50} determined at 0.0135 mg/mL. Then, the inhibition of α-glucosidase by TPCE intensified with increased concentrations, as depicted in Figure 5b. The inhibition rate improved from 22.22 ± 1.26 to 66.54 ± 1.53% as TPCE concentrations increased from 40 to 200 mg/mL, with an IC_{50} determined at 130.3 mg/mL. For the reaction of the positive control, the IC_{50} values of ACB on the α-amylase and α-glucosidase enzymes were 0.0113 mg/mL and 2.028 mg/mL, respectively.

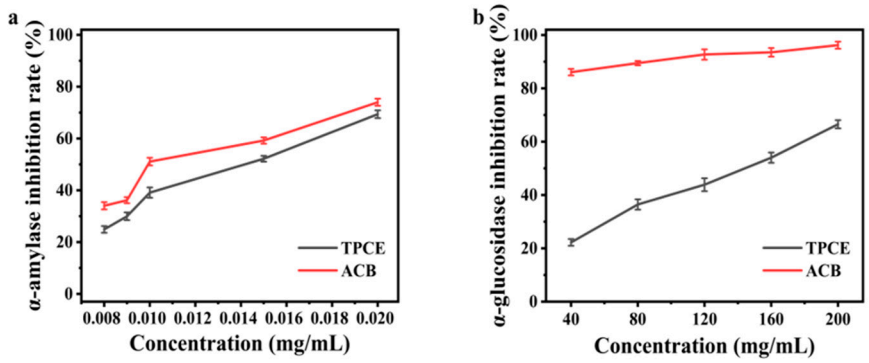


Figure 5. Inhibition of two enzymatic activities by different concentrations of TPCE. (**a**) α-amylase, (**b**) α-glucosidase.

The results demonstrated that TPCE exhibited favorable inhibitory activity against α-amylase, with IC_{50} data similar to that of the positive control drug. However, its inhibitory effect on α-glucosidase was weaker than that of the positive control. When compared with literature data for similar wild edible mushroom crude extracts, the IC_{50} values of TPCE against both α-amylase and α-glucosidase fell within the reported ranges for mushroom-derived hypoglycemic agents. Regarding the enzyme inhibitory activity, multiple compounds identified in TPCE and widely reported in the literature exerted potent

α-amylase and α-glucosidase inhibitory effects, including polysaccharides, phenolic derivatives, terpenoids, malic acid, and sugar alcohols, which are believed to act synergistically to contribute to the observed antidiabetic potential of TPCE [28,29]. TPCE, as a crude extract, exhibited IC_{50} against α-amylase very close to that of the positive control ACB, indicating its potent inhibitory activity against this enzyme. Given that TPCE is a crude extract while the positive control is a pure compound, these findings indicate that TPCE possesses potential for development as an antidiabetic agent. In future studies, we will further investigate the active monomers present in TPCE.

3. Materials and Methods

3.1. Reagents and Materials

Materials: Dried *H. erinaceus* from Jilin Province was crushed and sieved through an 80 mesh sieve. Folin–Ciocalteu reagent (10% (*v*/*v*)) and anhydrous ethanol analytical grade) were acquired from Beijing Chemical Reagent Co., Ltd. (Beijing, China). Gallic acid standard, L-ascorbic acid (Vc), ferrous sulfate, 2,2-Diphenyl-1-Picrylhydrazyl (DPPH), hydrogen peroxide, salicylic acid, 2,2′-Azinobis-(3-Ethylbenzthiazoline-6-Sulphonic acid) (ABTS), Acarbose (ACB), α-glucosidase, and α-amylase were purchased from Shanghai Yuanye Biotechnology Co., Ltd. (Shanghai, China). DNS reagent came from Beijing Soleberg Technology Co., Ltd. (Beijing, China).

Equipment: Numerical control ultrasonic cleaner (Kunshan Hechuang Ultrasonic Instrument Co., Ltd., Kunshan, China); Rotary evaporator (Heidolph, Schwabach, Germany); High-speed refrigerated centrifuge (Sigma, Cream Ridge, NJ, USA); Multifunctional microplate reader (Molecular Devices, San Jose, CA, USA); UHPLC-QTOF system (Agilent Technologies Co., Ltd., Santa Clara, CA, USA).

3.2. Optimization of Polyphenol Extraction Process

3.2.1. Polyphenol Standard Curve

Polyphenol content was quantified using a standard curve with gallic acid as the reference standard, the most widely adopted compound for Folin–Ciocalteu (F-C) total phenolic analysis due to its stability, consistent reactivity with F-C reagent, and common use in phytochemical studies [29]. Concentrations of 0.016–0.08 mg/L gallic acid standard solution were added. Another 0.5 mL of 10% F-C reagent and 1 mL of 10% Na_2CO_3 were added in sequence. Then, the solution was placed in the dark for 0.5 h, and the absorbance (A) was measured at a wavelength of 760 nm. The abscissa was taken as the solution concentration, and the ordinate was taken as the absorbance A_{760} to form a standard working curve [30].

3.2.2. Determination of Polyphenol Yield

Following extraction, the polyphenol yield from *H. erinaceus* was calculated according to the following formula [31]:

$$Y = (C \times V \times n/m) \times 100\% \quad (1)$$

where C is the mass concentration of *H. erinaceus* polyphenol calculated according to the absorption value, %; V is the total amount of *H. erinaceus* polyphenol extract volume, mL; m is the weight of *H. erinaceus*, mg; and n is the dilution ratio.

3.2.3. Effect of Solid–Liquid Ratio on Polyphenol Yield

Five parts of 1 g of *H. erinaceus* power were accurately weighed in a 100 mL Erlenmeyer flask, the extraction conditions were fixed, with an ethanol solvent of 60%, extraction time of 50 min, ultrasonic power of 400 W, and extraction temperature of 25 °C. Subsequently,

a single-factor test was conducted by adjusting the solid–liquid ratio. Each experiment was duplicated twice, and the two extracts were merged. The filtrate was concentrated under reduced pressure and djusted to 5 mL with 60% ethanol prior to the determination of polyphenol yield.

3.2.4. Effect of Extraction Time on Polyphenol Yield

After accurately weighing five aliquots of 1 g each of *H. erinaceus* power and transferring each aliquot to a 100 mL Erlenmeyer flask, the extraction conditions were kept constant: 60% ethanol was used as the extraction solvent, the solid–liquid ratio was set at 1:20 (g/mL), the ultrasonic power was fixed at 400 W, and the temperature was maintained at 25 °C. Subsequently, a single-factor experiment was performed by varying only the extraction time. Each experiment was duplicated twice, and the two extracts were merged. The filtrate was concentrated under reduced pressure, and djusted to 5 mL with 60% ethanol, prior to the determination of polyphenol yield.

3.2.5. Effect of Ethanol Concentration on Polyphenol Yield

Five 1 g aliquots of *H. erinaceus* power were precisely weighed, with each aliquot placed into a 100 mL Erlenmeyer flask; the extraction parameters were maintained at constant values: a solid–liquid ratio of 1:20 (g/mL), extraction duration of 50 min, ultrasonic power of 400 W, and ultrasonic temperature of 25 °C. A single-factor assay was then performed, where the only variable was the concentration of ethanol used for extraction. Each experiment was duplicated twice, and the two extracts were merged. The filtrate was concentrated under reduced pressure and djusted to 5 mL with 60% ethanol prior to the determination of polyphenol yield.

3.2.6. Polyphenol Extraction BBD Response Surface Method Experimental Design

The experimental scheme was obtained using Design-Expert 8.0 software and BBD. Based on the results of the one-factor test, the main factors with significant effects on polyphenol yield were selected, and according to the principle of Box–Behnken central combination experimental design, a three-factor, three-level central composite design was carried out with the polyphenol yield of *H. erinaceus* as the response value. The experiment was repeated three times, and the polyphenol yield response values were obtained and averaged for data analysis. As shown in Table 5, the experimental factors and levels used the fitted second-order polynomial model volume:

$$Y = \sum_{i=1}^{3} \beta_i X_i + \sum_{i=1}^{3} \beta_{ii} X_i^2 + \sum_{i=1}^{2} \sum_{j=i+1}^{3} \beta_{ij} X_i X_j$$

where Y is the predicted response; β_i, β_{ii} and β_{ij} are regression coefficients of intercept term, linear term, quadratic term and interaction term, respectively, and X_i and X_j are coding parameters.

Table 5. Response surface BBD experimental factors and levels.

Variables	Symbol	Coded Levels		
		−1	0	+1
Extraction time (min)	A	40	50	60
Solid–liquid ratio (g/mL)	B	40	50	60
Ethanol concentration (%)	C	30	40	50

3.3. LC-MS Analysis

LC-MS analysis was performed using an Agilent 1290II-6545 UHPLC-QTOF system, equipped with a Waters (Milford, MA, USA) ACQUITY UPLC BEH C_{18} (2.1 × 50 mm, 1.7 μm). The mobile phase consisted of two components; mobile phase A comprised 0.1% formic acid in water, while mobile phase B was 0.1% formic acid solution in acetonitrile. Data were collected in both positive and negative ionization modes. The full scan was conducted at 100 to 3000 m/z.

H. erinaceus extract was prepared using 80% methanol solution, filtered with a 0.22 μm microporous nylon membrane, and then evaluated.

3.4. Determination of Antioxidant Activity

3.4.1. $ABTS^{+}\cdot$ Radical Scavenging Assay

An $ABTS^{+}\cdot$ radical scavenging capacity assay was performed with minor modifications in reference to the method of Re et al. [32]. To evaluate the $ABTS^{+}\cdot$ radical scavenging capacity of TPCE, a reaction mixture consisting of 7 mM ABTS reagent and 140 mM potassium persulfate ($K_2S_2O_8$) was prepared. This mixture was then incubated in the dark at 4 °C for 12 h, to facilitate the generation of $ABTS^{+}\cdot$ radicals. Subsequently, 100 μL of TPCE samples with various concentrations were separately mixed thoroughly with 100 μL of the $ABTS^{+}\cdot$ stock solution. After standing in the dark for 30 min, the absorbance of each mixture was measured at a wavelength of 734 nm. Each group of experiments was performed in triplicate to ensure the reliability and reproducibility of the experimental results. The absorbance of the sample reaction system was denoted as A_i, while A_0 represented the absorbance measured by substituting the sample with the sample solvent. A_j was defined as the absorbance obtained when the $ABTS^{+}\cdot$ solution was replaced by the sample solvent. Vc served as the positive control, and the $ABTS^{+}\cdot$ radical scavenging activity was calculated by applying the following formula:

$$ABTS^{+\cdot} \text{ radical scavenging rate } = \left(1 - \left(A_i - A_j\right)/A_0\right) \times 100\% \quad (2)$$

3.4.2. $OH\cdot$ Radical Scavenging Assay

The free radical was determined using the method of Smirnof and Geng with minor modifications [33,34]. A volume of 50 μL TPCE sample solutions was mixed with 50 μL of 50 mmol/L ferrous sulfate ($FeSO_4$) solution, 50 μL of 10 mmol/L salicylic acid–ethanol solution, and 50 μL of 3% hydrogen peroxide (H_2O_2) solution. The resulting mixture was incubated in the dark for 30 min. Triplicate measurements were carried out for each experimental group to ensure the reliability and repeatability of the results. After the incubation period, the absorbance of reaction system (designated as $A_{reaction}$) was measured at a wavelength of 510 nm. For the control group ($A_{control}$), distilled water was used to replace the salicylic acid–ethanol solution, and the corresponding absorbance was recorded. For the blank group (A_{blank}), the sample was substituted with the sample solvent, and its absorbance was measured as well. Vc was employed as the positive control, and the $OH\cdot$ radical scavenging capacity was computed in accordance with the following formula:

$$OH^{\cdot} \text{ radical scavenging rate} = \left(1 - \frac{A_{reaction} - A_{control}}{A_{blank}}\right) \times 100\% \quad (3)$$

where $A_{reaction}$ represents the absorbance of the sample, $A_{control}$ represents the absorbance of the blank control group, and A_{blank} represents the absorbance of the sample without hydrogen peroxide.

3.4.3. DPPH· Radical Scavenging Assay

The experiments were carried out using the method described in Brand-Williams [35]. TPCE samples with different concentration gradients (100 μL each) were individually mixed with 100 μL of DPPH· solution. Each experimental group was run in triplicate to ensure that the experimental results were reliable and reproducible. After incubating the mixture for 30 min, the absorbance (denoted as A_i) was determined at a wavelength of 517 nm. The control absorbance values were recorded: A_j was measured by substituting the TPCE sample with the sample solvent, while A_c was obtained by replacing the DPPH· solution with anhydrous ethanol. Vc was used as the positive control, and the DPPH· radical scavenging capacity was calculated by means of the following formula:

$$\text{DPPH}\cdot \text{ clearance} = \left(1 - \left(A_i - A_j\right)/A_c\right) \times 100\% \quad (4)$$

3.5. Determination of Inhibition Rate

3.5.1. Determination of α-Amylase Inhibition Rate

The experiments were carried out using the method described in Padilla-Camberos, et al. [36]. TPCE solutions (0.008–0.020 mg/mL) in volumes of 100 μL were mixed with 50 μL of α-amylase (1.0 U/mL); following a 15 min incubation period at 37 °C, 50 μL of 1% (*w*/*v*) soluble starch was added, and the solutions were then incubated for a further 10 min. Subsequently, 100 μL of DNS was introduced into the mixture, and then heated at 100 °C for 5 min. After cooling, 1 mL of distilled water was added, and the absorbance at 540 nm was measured. Each experimental group was run in triplicate to ensure that the experimental results were reliable and reproducible. The inhibition rate was calculated using the following equation:

$$\text{Inhibition rate} = \left(1 - \left(A_1 - A_2\right)/\left(A_0 - A_0'\right)\right) \times 100\% \quad (5)$$

where A_1, A_2, A_0, and A_0 are the absorbances at 540 nm for the sample group, blank sample group, control group, and blank control group, respectively. IC_{50} was determined from the regression equation of the inhibition curve.

3.5.2. Determination of α-Glucosidase Inhibition Rate

The experiments were carried out using the method described in Yao et al. [37]. TPCE solutions (5–160 mg/mL) in volumes of 100 μL were mixed with 50 μL of α-glucosidase solution (0.5 U/mL). The mixture was subsequently incubated at 37 °C for 15 min. Subsequently, 100 μL of PNPG (5.0 mmol/L) was added to the reaction mixture, which was then incubated at 37 °C for 10 min. The reaction was terminated by the addition of 750 μL of Na_2CO_3 (1.0 mol/L), and the absorbance was recorded at 405 nm. Triplicate measurements were carried out for each experimental group to ensure the reliability and repeatability of the results. The inhibition rate was calculated using the following equation:

$$\text{Inhibition rate} = \left(1 - \left(A_1 - A_2\right)/\left(A_0 - A_0'\right)\right) \times 100\% \quad (6)$$

where A_1, A_2, A_0, and A_0 are the absorbances at 405 nm for the sample group, blank sample group, control group, and blank control group, respectively. IC_{50} was determined from the regression equation of the inhibition curve.

4. Conclusions

In this research, ultrasound-assisted extraction was employed to extract polyphenols from *H. erinaceus*, and the effects of extraction duration, solid–liquid ratio, and ethanol concentration on polyphenol yield were systematically evaluated. Subsequent optimization

via BBD response surface methodology determined the optimal extraction parameters: extraction time of 56.85 min, solid–liquid ratio of 1:56.71 g/mL, and ethanol concentration of 44.64%, under which the TPCE yield reached 0.9985 ± 0.03%, verifying the effectiveness and reproducibility of the optimized extraction protocol for *H. erinaceus* polyphenols. In addition, LC-MS analysis tentatively identified multiple bioactive constituents in TPCE (including polysaccharides, phenolics, terpenoids, malic acid, and sugar alcohols), laying a preliminary chemical foundation for the observed bioactivities. In vitro bioactivity assessments revealed that TPCE possessed notable free radical scavenging capacity, with the potency ranking $ABTS^{+}\cdot$ > ·OH > DPPH·, corresponding to EC_{50} values of 0.8850 mg/mL, 0.9490 mg/mL, and 4.198 mg/mL, respectively. Furthermore, TPCE exhibited remarkable inhibitory activity against carbohydrate-digesting enzymes, with IC_{50} values of 0.0135 mg/mL for α-amylase and 130.3 mg/mL for α-glucosidase; the IC_{50} of ACB on α-amylase was 0.0113 mg/mL, indicating that TPCE possesses favorable inhibitory activity against α-amylase. Collectively, these quantitative and qualitative findings provide robust scientific evidence supporting the nutritional and medicinal value of *H. erinaceus* and highlight its promising application potential as a natural adjudicative agent for blood glucose regulation and oxidative stress relief.

Author Contributions: Methodology, S.P.; Formal analysis, L.C.; Investigation, H.L., S.P. and Y.S.; Writing—original draft, H.L. and C.Z.; Writing—review and editing, J.W.; Visualization, H.L. and C.Z.; Supervision, L.C., J.W. and H.B. All authors have read and agreed to the published version of the manuscript.

Funding: This research was supported by the Natural Science Foundation of Changchun Normal University (CSJJ2025003ZK) and the Natural Science Foundation of Jilin Province (YDZJ202601ZYTS266).

Institutional Review Board Statement: This research exclusively focuses on the extraction, isolation, and bioactivity evaluation of bioactive compounds from *Hericium erinaceus*; no studies involving human subjects, animal testing, or clinical samples were performed by any of the authors.

Informed Consent Statement: Not applicable.

Data Availability Statement: Data are contained within the article.

Acknowledgments: The authors gratefully acknowledge the technical support provided by the National Local Joint Engineering Laboratory for Natural Medicine Separation, Purification and Activity Screening Technology, and Jilin Provincial Innovation Laboratory for Research and Development of Cold-Region Economic Plants and Edible-Medicinal Fungi.

Conflicts of Interest: The authors declare no conflict of interest.

References

1. Soković, M.; Glamočlija, J.; Ćirić, A.; Petrović, J.; Stojković, D. Mushrooms as sources of therapeutic foods. In *Therapeutic Foods*; Academic Press: Cambridge, MA, USA, 2018; pp. 141–178. [CrossRef]
2. Nguyen, B.T.; Ngo, N.; Le, V.; Nguyen, L.; Tran, A.; Nguyen, L.H. Identification of Optimal Culture Conditions for Mycelial Growth and Cultivation of Monkey Head Mushrooms (*Hericium erinaceus* (Bull.: fr.) Pers). *Vietnam. J. Agric. Sci.* **2018**, *1*, 117–126. [CrossRef]
3. Wang, F.; Wang, K.; Cai, L.; Zhao, M.; Kirk, P.M.; Fan, G.; Sun, Q.; Li, B.; Wang, S.; Yu, Z. Fungal names: A comprehensive nomenclatural repository and knowledge base for fungal taxonomy. *Nucleic Acids Res.* **2023**, *51*, D708–D716. [CrossRef]
4. Deshmukh, S.K.; Sridhar, K.R.; Gupta, M.K. *Hericium erinaceus*—A Rich Source of Diverse Bioactive Metabolites. *Fungal Biotechnol.* **2021**, *1*, 10–38. [CrossRef]
5. Qiu, Y.; Lin, G.; Liu, W.; Zhang, F.; Linhardt, R.J.; Wang, X.; Zhang, A. Bioactive compounds in *Hericium erinaceus* and their biological properties: A review. *Food Sci. Hum. Wellness* **2024**, *13*, 1825–1844. [CrossRef]
6. Thongbai, B.; Rapior, S.; Hyde, K.D.; Wittstein, K.; Stadler, M. *Hericium erinaceus*, an amazing medicinal mushroom. *Mycol. Prog.* **2015**, *14*, 91. [CrossRef]

7. Pan, F.; Liu, X.; Qiao, M.; Liu, J.; Pang, Y.; Zhang, M.; Yu, W. Innovative composite systems for enhancing plant polyphenol stability and bioavailability. *Food Sci. Biotechnol.* **2025**, *34*, 1819–1834. [CrossRef] [PubMed]
8. Asfaw, D.E. Antioxidant Properties of Phenolic Compounds to Manage Oxidative Stress/A Review. *J. Adv. Agron. Crop* **2023**, *1*, 1–16. [CrossRef]
9. Banwo, K.; Olojede, A.O.; Adesulu-Dahunsi, A.T.; Verma, D.K.; Thakur, M.; Tripathy, S.; Singh, S.; Patel, A.R.; Gupta, A.K.; Aguilar, C.N.; et al. Functional importance of bioactive compounds of foods with Potential Health Benefits: A review on recent trends. *Food Biosci.* **2021**, *43*, 101320. [CrossRef]
10. de Camargo, A.C.; Schwember, A.R. Phenolic-driven sensory changes in functional foods. *J. Food Bioact.* **2019**, *5*, 6–7. [CrossRef]
11. Sevindik, M.; Gürgen, A.; Khassanov, V.T.; Bal, C. Biological Activities of Ethanol Extracts of *Hericium erinaceus* Obtained as a Result of Optimization Analysis. *Foods* **2024**, *13*, 1560. [CrossRef]
12. Szydłowska-Tutaj, M.; Szymanowska, U.; Tutaj, K.; Domagała, D.; Złotek, U. The addition of reishi and lion's mane mushroom powder to pasta influences the content of bioactive compounds and the antioxidant, potential anti-inflammatory, and anticancer properties of pasta. *Antioxidants* **2023**, *12*, 738. [CrossRef]
13. Li, H.; Park, S.; Moon, B.; Yoo, Y.B.; Lee, Y.W.; Lee, C. Targeted phenolic analysis in *Hericium erinaceum* and its antioxidant activities. *Food Sci. Biotechnol.* **2012**, *21*, 881–888. [CrossRef]
14. Darmasiwi, S.; Aramsirirujiwet, Y.; Kimkong, I. Antibiofilm activity and bioactive phenolic compounds of ethanol extract from the *Hericium erinaceus* basidiome. *J. Adv. Pharm. Technol. Res.* **2022**, *13*, 111–116. [CrossRef]
15. Ruangchuay, S.; Wang, Q.Q.; Wang, L.Y.; Lin, J.; Wang, Y.C.; Zhong, G.H.; Maneenoon, K.; Huang, Z.B.; Chusri, S. Antioxidant and antiaging effect of traditional Thai rejuvenation medicines in Caenorhabditis elegans. *J. Integr. Med.* **2021**, *19*, 362–373. [CrossRef]
16. Machado-Carvalho, L.; Martins, T.; Aires, A.; Marques, G. Optimization of phenolic compounds extraction and antioxidant activity from Inonotus hispidus using ultrasound-assisted extraction technology. *Metabolites* **2023**, *13*, 524. [CrossRef]
17. Wu, X.Q.; Ding, H.F.N.; Hu, X.; Pan, J.H.; Liao, Y.J.; Gong, D.; Zhang, G.W. Exploring inhibitory mechanism of gallocatechin gallate on a-amylase and a-glucosidase relevant to postprandial hyperglycemia. *J. Funct. Foods* **2018**, *48*, 200–209. [CrossRef]
18. Dzah, C.S.; Duan, Y.Q.; Zhang, H.H.; Wen, C.T.; Chen, G.Y.; Ma, H.L. The effects of ultrasound assisted extraction on yield, antioxidant, anticancer and antimicrobial activity of polyphenol extracts: A review. *Food Biosci.* **2020**, *35*, 100547. [CrossRef]
19. Abugri, D.A.; McElhenney, W.H. Extraction of total phenolic and flavonoids from edible wild and cultivated medicinal mushrooms as affected by different solvents. *J. Nat. Prod. Plant Resour.* **2013**, *3*, 37–42.
20. Takeuchi, T.M.; Pereira, C.G.; Braga, M.E.; Maróstica, M.R.; Leal, P.F.; Meireles, M.A.A. Low-pressure solvent extraction (solid–liquid extraction, microwave assisted, and ultrasound assisted) from condimentary plants. In *Extracting Bioactive Compounds for Food Products*; CRC Press: Boca Raton, FL, USA, 2008; pp. 137–218. [CrossRef]
21. Naz, R.; Saqib, F.; Awadallah, S.; Wahid, M.; Latif, M.F.; Iqbal, I.; Mubarak, M.S. Food Polyphenols and Type II Diabetes Mellitus: Pharmacology and Mechanisms. *Molecules* **2023**, *28*, 3996. [CrossRef] [PubMed]
22. Li, X.X.; Bai, Y.X.; Jin, Z.Y.; Svensson, B. Food-derived non-phenolic α-amylase and α-glucosidase inhibitors for controlling starch digestion rate and guiding diabetes-friendly recipes. *LWT* **2022**, *153*, 112455. [CrossRef]
23. Husain, A.; Khanam, A.; Alouffi, S.; Shahab, U.; Alharazi, T.; Maarfi, F.; Khan, S.; Hasan, Z.; Akasha, R.; Farooqui, A.; et al. C-phycocyanin from cyanobacteria: A therapeutic journey from antioxidant defence to diabetes management and beyond. *Phytochem. Rev.* **2024**, *24*, 4489–4507. [CrossRef]
24. Hu, D.B.; Xue, R.; Zhuang, X.C.; Zhang, X.S.; Shi, S.L. Ultrasound-assisted extraction optimization of polyphenols from *Boletus bicolor* and evaluation of its antioxidant activity. *Front. Nutr.* **2023**, *10*, 1135712. [CrossRef] [PubMed]
25. Rahimah, S.B.; Djunaedi, D.D.; Soeroto, A.Y.; Bisri, T. The Phytochemical Screening, Total Phenolic Contents and Antioxidant Activities In Vitro of White Oyster Mushroom (*Pleurotus ostreatus*) Preparations. *Open Access Maced. J. Med. Sci.* **2019**, *7*, 2404–2412. [CrossRef]
26. Rajendra Prasad, R.P.; Varshney, V.K.; Harsh, N.S.K.; Manoj Kumar, M.K. Antioxidant capacity and total phenolics content of the fruiting bodies and submerged cultured mycelia of sixteen higher Basidiomycetes mushrooms from India. *Int. J. Med. Mushrooms* **2015**, *17*, 933–941. [CrossRef]
27. Ramesh, C.H.; Pattar, M.G. Antimicrobial properties, antioxidant activity and bioactive compounds from six wild edible mushrooms of western ghats of Karnataka. *Pharmacogn. Res.* **2010**, *2*, 107. [CrossRef]
28. Deveci, E.; Çayan, F.; Tel-Çayan, G.; Duru, M.E. Inhibitory activities of medicinal mushrooms on α-amylase and α-glucosidase-enzymes related to type 2 diabetes. *S. Afr. J. Bot.* **2021**, *137*, 19–23. [CrossRef]
29. Das, A.; Chen, C.M.; Mu, S.C.; Yang, S.H.; Ju, Y.M.; Li, S.C. Medicinal components in edible mushrooms on diabetes mellitus treatment. *Pharmaceutics* **2022**, *14*, 436. [CrossRef]
30. Singleton, V.L.; Rossi, J.A. Colorimetry of total phenolics with phosphomolybdic-phosphotungstic acid reagents. *Am. J. Enol. Vitic.* **1965**, *16*, 144–158. [CrossRef]
31. Liu, C.; Gong, F.; Chen, Y.; Xiong, Z.; Wang, C.; Li, J.; Guo, J. Comparison and Optimization of Three Extraction Methods for Epimedium polysaccharides. *Separations* **2024**, *11*, 296. [CrossRef]

32. Re, R.; Pellegrini, N.; Proteggente, A.; Pannala, A.; Yang, M.; Rice-Evans, C. Antioxidant activity applying an improved ABTS radical cation decolorization assay. *Free. Radic. Biol. Med.* **1999**, *26*, 1231–1237. [CrossRef] [PubMed]
33. Smirnoff, N.; Cumbes, Q.J. Hydroxyl radical scavenging activity of compatible solutes. *Phytochemistry* **1989**, *28*, 1057–1060. [CrossRef]
34. Geng, M.J.; Ren, M.X.; Liu, Z.L.; Shang, X.J. Free radical scavenging activities of pigment extract from *Hibiscus syriacus* L. petals in vitro. *Afr. J. Biotechnol.* **2012**, *11*, 429–435. [CrossRef]
35. Brand-Williams, W.; Cuvelier, M.E.; Berset, C. Use of a Free Radical Method to Evaluate Antioxidant Activity. *LWT—Food Sci. Technol.* **1995**, *28*, 25–30. [CrossRef]
36. Padilla-Camberos, E.; Lazcano-Díaz, E.; Flores-Fernandez, J.M.; Owolabi, M.S.; Allen, K.; Villanueva-Rodríguez, S. Evaluation of the Inhibition of Carbohydrate Hydrolyzing Enzymes, the Antioxidant Activity, and the Polyphenolic Content of *Citrus limetta* Peel Extract. *Sci. World J.* **2014**, *2014*, 121760. [CrossRef]
37. Yao, M.; Liu, J.; Zhou, F.; Li, H.; Wang, R.; Han, Z.; Liu, J.; Chen, W.; Liu, G.; Yang, S.; et al. α-Glucosidase inhibitory activity of polyphenol-rich sugarcane extract: Screening and mechanistic insights based on biolayer interferometry-mass spectrometry. *Front. Nutr.* **2025**, *12*, 1575409. [CrossRef] [PubMed]

Disclaimer/Publisher's Note: The statements, opinions and data contained in all publications are solely those of the individual author(s) and contributor(s) and not of MDPI and/or the editor(s). MDPI and/or the editor(s) disclaim responsibility for any injury to people or property resulting from any ideas, methods, instructions or products referred to in the content.